

# Electron-Pair Excitations and the Molecular Coulomb Continuum

J. M. Feagin,<sup>1</sup> J. Colgan,<sup>2</sup> A. Huetz,<sup>3</sup> T. Reddish<sup>4\*</sup>

<sup>1</sup>*Department of Physics, California State University-Fullerton, Fullerton, CA 92834, USA*

<sup>2</sup>*Theoretical Division, Los Alamos National Laboratory, Los Alamos, New Mexico 87545, USA*

<sup>3</sup>*CNRS, Université Paris-Sud, LIXAM UMR8624, Bâtiment 350, Orsay, Cedex, F-91405, France*

<sup>4</sup>*Department of Physics, University of Windsor, 401 Sunset Avenue, Ontario, Canada, N9B 3P4*

(Dated: February 16, 2009)

Electron-pair excitations in the molecular hydrogen continuum are described by quantizing rotations of the momentum plane of the electron pair about the pair's relative momentum. A helium-like description of the molecular photo double ionization is thus extended to higher angular momenta of the electron pair. A simple three-state superposition is found to account surprisingly well for recent observations of noncoplanar electron-pair, molecular-axis angular distributions.

PACS numbers: 33.80.Eh, 34.10.+x

One of the surprises of early observations of photo double ionization of molecular hydrogen was the close similarity with the corresponding electron-pair angular distributions well established in helium, especially for relatively low-energy electron pairs [1]. The helium (free-atom) double ionization angular distributions, viz. the triple differential cross sections TDCS, have a remarkably simple form for equal energy ejected electrons, namely,

$$\text{TDCS} \sim |\hat{\epsilon} \cdot \mathbf{k}_1 + \hat{\epsilon} \cdot \mathbf{k}_2|^2 = |\hat{\epsilon} \cdot \mathbf{k}_+|^2, \quad (1)$$

with  $\hat{\epsilon}$  the photon polarization. Here,  $\hbar \mathbf{k}_+ = \hbar \mathbf{k}_1 + \hbar \mathbf{k}_2$  is the momentum of the photoejected electron-pair center of mass. The simplicity of this result derives from the underlying  $^1S^e \rightarrow ^1P^o$  dipole excitation. In molecular dipole excitation, the geometry of the molecule naturally resolves the photon polarization into components parallel ( $\Sigma$ ) and perpendicular ( $\Pi$ ) to the relative momentum direction  $\mathbf{K}_- \equiv (\mathbf{K}_1 - \mathbf{K}_2)/2$  of the Coulomb-exploding ion pair [2], so that

$$\hat{\epsilon} \rightarrow \epsilon_\Pi + \epsilon_\Sigma = \sin \theta_N \hat{\epsilon}_\Pi + \cos \theta_N \hat{\mathbf{K}}_-. \quad (2)$$

Thus, with the helium-like amplitude  $\hat{\epsilon} \cdot \mathbf{k}_+$  from Eq. (1), one obtains an approximate *molecular* double ionization distribution or fully differential cross section FDCS for equal-energy ejected electrons according to

$$\text{FDCS} = |a_\Pi \sin \theta_N \hat{\epsilon}_\Pi \cdot \mathbf{k}_+ + a_\Sigma \cos \theta_N \hat{\mathbf{K}}_- \cdot \mathbf{k}_+|^2, \quad (3)$$

where the  $a_\Lambda$  are undetermined dipole amplitudes internal to the molecule but independent of the momenta of the ionization fragments. This expression helps to explain the observed close similarity of low-energy helium and molecular hydrogen angular distributions. It is readily extended to unequal energy sharing and thus gives remarkably good fits to a variety of data, especially for coplanar geometries with respect to the ion- and electron-pair momenta and photon polarization.

Gisselbrecht et al. recently identified, however, equal-energy-sharing electron-pair configurations in the molecular fragmentation for which the helium-like description

categorically fails [3]. Their observations follow on from earlier experiments by Weber et al. [4]. These anomalous angular distributions are noncoplanar and occur when one electron is observed perpendicular to the plane of the other and the polarization direction with the ion-pair direction  $\mathbf{K}_-$  either parallel or perpendicular to the polarization. Gisselbrecht et al. termed these and related configurations *frozen-correlation*, since the electron-pair angular separation  $\hat{\mathbf{k}}_1 \cdot \hat{\mathbf{k}}_2$  is held fixed in all three cases.

Parallel to these experimental achievements and insights, the community has seen decisive advancement in the *ab initio* computation of Coulomb few-body fragmentation, in particular from two groups, one using a time-independent close-coupling approach with exterior complex scaling (ECS) [5], and one using a time-dependent close-coupling approach (TDCC) [6]. Their abundant 'virtual data' are in excellent agreement in both magnitude and angular distribution with a wide variety of experimentally measured cross sections for both the coplanar and noncoplanar geometries. Results of the TDCC calculation [6] for these three distributions are shown in Fig. 1, and when folded over the experimental angular acceptances agree well with experiment (see the insets).

For each of these three configurations, one readily sees that Eq. (3) predicts the same simple  $\mathbf{k}_2$  angular distribution of one electron, namely  $\text{FDCS} \sim (\hat{\epsilon} \cdot \hat{\mathbf{k}}_2)^2 \equiv \cos^2 \theta_2$  with respect to a laboratory  $z_L$  axis along  $\hat{\epsilon}$  and a  $y_L$  axis along  $\mathbf{k}_1$  of the other electron held fixed perpendicular to the  $\mathbf{k}_2, \hat{\epsilon}$  plane. Thus, although Fig. 1a with ion-pair direction  $\mathbf{K}_-$  held fixed along  $\mathbf{k}_1$  shows good agreement with the helium-like  $\cos^2 \theta_2$  description, Figs. 1b and 1c show increasing deviations which become especially strong in Fig. 1c with  $\mathbf{K}_-$  held fixed along  $\hat{\epsilon}$ .

One is thus lead to reconsider the helium-like description of molecular fragmentation and the role of higher angular momentum contributions to the electron pairs. In the molecular ground state, the electron-pair total angular momentum  $\mathbf{L} = \mathbf{l}_1 + \mathbf{l}_2$  is not a good quantum number, so the helium-like dipole selection rule  $^1S^e \rightarrow ^1P^o$  generalizes to  $^1S^e, ^1P^e, ^1D^e, \dots \rightarrow ^1P^o, ^1D^o, ^1F^o, \dots$  (the

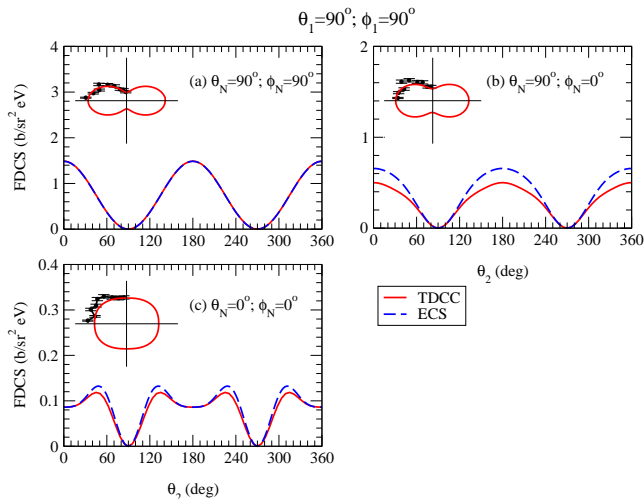


FIG. 1:  $H_2$  photo double ionization cross sections computed using time-dependent (TDCC) [6] and time-independent (ECS) [5] close coupling as a function of the orientation  $\theta_2$  of the momentum direction  $\mathbf{k}_2$  of one electron relative to a laboratory  $z_L$  axis along the polarization direction  $\hat{\epsilon}$  for 25 eV electron pairs with equal energy sharing. In each plot, the momentum direction  $\mathbf{k}_1$  of the other electron is aligned along a  $y_L$  axis perpendicular to the  $\mathbf{k}_2, \hat{\epsilon}$  plane. The three plots (a), (b) and (c) thus show three orientations  $\theta_N, \phi_N$  of the ion-pair direction  $\mathbf{K}_-$  along the three axes  $y_L, x_L$  and  $z_L$ , respectively. The polar-plot insets show a folded comparison with the experimental measurements of Gisselbrecht et al. [3].

exchange and parity dipole selection rules remain the same).

Based on our longtime experience with electron-pair excitations in helium and  $H^-$ , it turns out to be advantageous—perhaps surprisingly so—to define states of total  $L$  by quantizing rotations of the momentum plane of the electron pair, depicted in Fig. 2, based on a  $z$  axis along their relative momentum direction  $\mathbf{k}_- = (\mathbf{k}_1 - \mathbf{k}_2)/2$ . One thus introduces symmetric-top wavefunctions  $\tilde{D}_{Mm}^L(\hat{\mathbf{k}}_-)$  defined by projections  $\hbar m = \mathbf{L} \cdot \hat{\mathbf{k}}_-$  and  $\hbar M = \mathbf{L} \cdot \hat{\mathbf{z}}_M$ , where  $\hat{\mathbf{z}}_M$  is a *molecular-frame*  $z$  axis, which we will take here to be along the ion-pair relative momentum direction  $\mathbf{K}_-$ .

One thus constructs electron-pair *momentum* states of definite  $LS\pi^e$  symmetry for  $L \geq 1$  according to

$$\begin{aligned} \tilde{\psi}_M^{(2S+1)L\lambda} &= \tilde{\phi}_\lambda(\mathbf{k}_+, k_-) \\ &\times \left[ \tilde{D}_{M\lambda}^L(\hat{\mathbf{k}}_-) + \pi^e(-)^{L+\lambda} \tilde{D}_{M-\lambda}^L(\hat{\mathbf{k}}_-) \right], \end{aligned} \quad (4)$$

where  $\lambda \equiv |m|$  and  $\tilde{\phi}_\lambda(\mathbf{k}_+, k_-)$  is an internal state of the electron pair that describes only the relative orientation of the pair within the rotating  $\mathbf{k}_1, \mathbf{k}_2$  plane and thus depends on  $\mathbf{k}_+$  and only the magnitude  $k_- = |\mathbf{k}_-|$ .

Although the analytic form of the internal wavefunction remains unknown (the few-body Coulomb problem remains unsolved), the decomposition of electron-pair

states into symmetric-top wavefunctions has been used with good success to interpret and correlate a variety of observed dynamical symmetries and propensity rules in the doubly excited spectrum of helium and  $H^-$  both above and below the double ionization threshold [7].

For example, one can show quite generally [8] that the internal states have an internal *inversion* symmetry and therefore nodes as a function of  $k_{+z} \equiv \mathbf{k}_+ \cdot \hat{\mathbf{k}}_-$ , viz.  $\tilde{\phi}_\lambda(-k_{+z}) = \pi^e(-)^{S+\lambda} \tilde{\phi}_\lambda(k_{+z})$ , so that in the case of equal energy sharing of interest here with  $\mathbf{k}_+ \cdot \mathbf{k}_- = E_1 - E_2 = 0$ , the dipole-allowed (*singlet*,  $\pi^e = \text{odd}$ ) internal states with  $\lambda = \text{even}$  vanish identically, i.e.  $\tilde{\phi}_{\lambda=\text{even}}(E_1 = E_2) \equiv 0$ , for a given  $L \geq \lambda$ . For unequal energy sharing, these states will be weakly populated, and we have an example of a propensity rule.

In the case of dipole-allowed molecular fragmentation with linearly polarized photons, we have the usual selection rules  ${}^1\Sigma_g^+ \rightarrow {}^1\Lambda_u^+$  with  $\Lambda \equiv |M| = 0, 1$  only and therefore to consider just the two sets of states  ${}^1\Sigma_u^+$  and  ${}^1\Pi_u^+$  for any given  $L$ . We thus require the electron-pair states in Eq. (4) all to have *ungerade* (*u*) molecular symmetry under ion exchange  $\mathbf{K}_- \rightarrow -\mathbf{K}_-$  which one readily shows is satisfied by taking  $\pi^e = \text{odd}$ . We also require an additional *even* (*+*) symmetry with respect to reflections in the  $\epsilon, \mathbf{K}_-$  plane [9]. One finds that the states in Eq. (4) reflect according to  $\tilde{\psi}_M \rightarrow \pi^e(-)^{L+M} \tilde{\psi}_{-M}$ . Thus, the dipole allowed  $\Lambda \equiv |M| = 0$   ${}^1\Sigma_u^+$  states have  $L = \text{odd}$  only. In particular, the  ${}^1\Sigma_u^+$  states with  $L = \text{even}$  are dipole forbidden. For  $\Lambda > 0$ , one must define in the usual way additional ‘ $\Lambda$ -doublet’ linear combinations

$$\tilde{\psi}_{\Lambda+} = \frac{1}{\sqrt{2}} \left[ \tilde{\psi}_\Lambda + \pi^e(-)^{L+\Lambda} \tilde{\psi}_{-\Lambda} \right], \quad (5)$$

which have even reflection symmetry for all  $L$ .

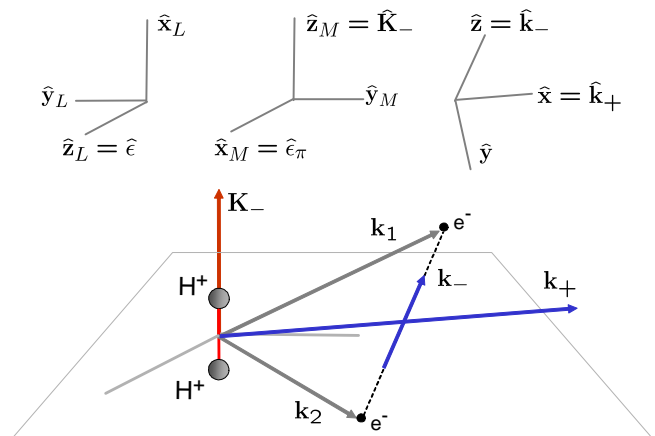


FIG. 2: Rotating  $\mathbf{k}_1, \mathbf{k}_2$  plane of an ejected electron pair following the photo fragmentation of molecular hydrogen. Here,  $\mathbf{k}_+ = \mathbf{k}_1 + \mathbf{k}_2$  and  $\mathbf{k}_- = (\mathbf{k}_1 - \mathbf{k}_2)/2$  refer to the electron pair, and  $\mathbf{K}_- = (\mathbf{K}_1 - \mathbf{K}_2)/2$  to the ion pair. The top three insets illustrate the three frames of reference used in the text. Left to right: laboratory, molecular, electron-pair.

We are now in a position to generalize to  $L > 1$  electron pairs the helium-like description of molecular fragmentation embodied in Eq. (3) by combining allowed  ${}^1\Sigma_u^+$  and  ${}^1\Pi_u^+$  states. We thus define dipole-allowed momentum states of an electron pair ejected into the molecular continuum according to

$$\begin{aligned} \tilde{\psi} = & \sum_{L \geq 1} \sum_{\lambda \leq L} a_{L\Pi\lambda} \sin \theta_N \tilde{\psi}_{\Pi^+}({}^1L_\lambda) \\ & + a_{2L-1,\Sigma\lambda} \cos \theta_N \tilde{\psi}_{\Sigma^+}({}^1(2L-1)_\lambda), \end{aligned} \quad (6)$$

where as before  $\cos \theta_N = \hat{\mathbf{K}}_- \cdot \hat{\boldsymbol{\epsilon}}$  and the  $a_{L\Lambda\lambda}$  are undetermined dipole amplitudes describing the internal molecular excitation dynamics but independent of the momenta of the ionization fragments.

To connect our expansion Eq. (6) with Eq. (3), it is convenient to express the symmetric-top wavefunctions  $\hat{D}_{\Lambda\lambda}^L(\hat{\mathbf{k}}_-)$  in an angle-independent fashion in terms of the direction cosines  $\hat{\mathbf{x}}_M \cdot \hat{\mathbf{x}}, \hat{\mathbf{y}}_M \cdot \hat{\mathbf{y}}, \hat{\mathbf{z}}_M \cdot \hat{\mathbf{z}}$ , etc. connecting the molecular and the electron-pair frames. Along with a  $z$  axis along  $\mathbf{k}_-$ , it is convenient here for equal-energy sharing,  $\mathbf{k}_+ \cdot \mathbf{k}_- = 0$ , to take the electron-pair-frame  $x$  axis along  $\mathbf{k}_+$  and thus  $y$  axis along  $\mathbf{k}_- \times \mathbf{k}_+ = \mathbf{k}_1 \times \mathbf{k}_2$  (see Fig. 2). We keep the molecular frame  $z_M$  axis along  $\mathbf{K}_-$  with  $\hat{\mathbf{z}}_M = \hat{\mathbf{K}}_- = \hat{\boldsymbol{\epsilon}}_\Sigma$  and take  $\hat{\mathbf{x}}_M = \hat{\boldsymbol{\epsilon}}_\Pi$  [cf. Eq. (2)], so that  $\hat{\mathbf{y}}_M = \hat{\mathbf{K}}_- \times \hat{\boldsymbol{\epsilon}}_\Pi$ .

With the frame axes thus defined in terms of the momentum vectors, we obtain the first three  $L$  contributions to Eq. (6) in a form analogous to Eq. (3) describing the dipole-allowed molecular states of the equal-energy electron-pair continuum according to

$$\begin{aligned} \tilde{\psi}({}^1P_{\lambda=1}) & \sim a_{1\Pi 1} \sin \theta_N \hat{\boldsymbol{\epsilon}}_\Pi \cdot \mathbf{k}_+ + a_{1\Sigma 1} \cos \theta_N \hat{\mathbf{K}}_- \cdot \mathbf{k}_+, \\ \tilde{\psi}({}^1D_{\lambda=1}) & \sim a_{2\Pi 1} \sin \theta_N \\ & \times \left( \hat{\boldsymbol{\epsilon}}_\Pi \cdot \mathbf{k}_+ - 2\hat{\mathbf{K}}_- \cdot \hat{\mathbf{k}}_- \hat{\mathbf{y}}_M \cdot \hat{\mathbf{k}}_- \times \mathbf{k}_+ \right), \\ \tilde{\psi}({}^1F_{\lambda=1}) & \sim a_{3\Pi 1} \sin \theta_N \\ & \times \left[ \left( 15(\hat{\mathbf{K}}_- \cdot \hat{\mathbf{k}}_-)^2 - 1 \right) \hat{\boldsymbol{\epsilon}}_\Pi \cdot \mathbf{k}_+ \right. \\ & \left. - 10\hat{\mathbf{K}}_- \cdot \hat{\mathbf{k}}_- \hat{\mathbf{y}}_M \cdot \hat{\mathbf{k}}_- \times \mathbf{k}_+ \right] \\ & + a_{3\Sigma 1} \cos \theta_N \left( 1 - 5(\hat{\mathbf{K}}_- \cdot \hat{\mathbf{k}}_-)^2 \right) \hat{\mathbf{K}}_- \cdot \mathbf{k}_+, \end{aligned} \quad (7)$$

where we have dropped miscellaneous normalization constants. We have also introduced the analytic (Wannier) threshold limit  $E_1 = E_2 = E/2 \rightarrow 0$  [8] for the internal wavefunctions,  $\tilde{\phi}_{\lambda=\text{odd}} \sim k_+^\lambda \sim E^{\lambda/2}$ , which suggests the  ${}^1F_{\lambda=1}$  state is favored in the low-energy spectrum over the allowed  ${}^1F_{\lambda=3}$  mode, which will be presented elsewhere. Recall that the  ${}^1P_{\lambda=0}$  as well as the  ${}^1D_{\lambda=0,2}$  contributions are *internal-inversion* forbidden for equal-energy sharing.

These results are readily applied to the frozen-correlation (fixed  $\hat{\mathbf{k}}_1 \cdot \hat{\mathbf{k}}_2$ ) configurations of Fig. 1 defined

relative to a laboratory  $z_L$  axis along the polarization direction  $\hat{\boldsymbol{\epsilon}}$  and a  $y_L$  axis along the momentum direction  $\mathbf{k}_1$  of one electron held fixed perpendicular to the  $\mathbf{k}_2$ ,  $\hat{\boldsymbol{\epsilon}}$  plane of the other. Superposing the three states in Eq. (7) thus gives the generalization of the molecular fragmentation distribution Eq. (3) according to

$$\text{FDCS} = N \cos^2 \theta_2 \left| 1 + B(\theta_N, \phi_N) \sin^2 \theta_2 \right|^2, \quad (8)$$

with  $\cos \theta_2 = \hat{\boldsymbol{\epsilon}} \cdot \hat{\mathbf{k}}_2$ . Here,  $N$  is a normalization constant while  $B(\theta_N, \phi_N)$  is a ratio involving the various amplitudes  $a_{L \leq 3, \Lambda 1}$  but independent of  $\theta_2$ .

For the configuration in Fig. 1a with  $\mathbf{K}_-$  held fixed parallel to  $\mathbf{k}_1$  along the  $y_L$  axis, we thus find in fact that  $B \equiv 0$ , so that Eq. (8) reduces to the pure  $\cos^2 \theta_2$  dependence observed [10]. For the configurations in Fig. 1b with  $\hat{\mathbf{K}}_- = \hat{\mathbf{x}}_L$  and in Fig. 1c with  $\hat{\mathbf{K}}_- = \hat{\mathbf{z}}_L = \hat{\boldsymbol{\epsilon}}$ , we find that  $B \propto a_{3\Pi 1}$  and  $B \propto a_{3\Sigma 1}$ , respectively, giving the additional  $\sin^2 \theta_2$  dependence in Eq. (8). In Fig. 1c for the pure  ${}^1\Sigma_g^+ \rightarrow {}^1\Sigma_u^+$  transition, there is no  ${}^1D_{\lambda=1}$  contribution [11]. We have thus fitted Eq. (8) to the TDCC calculations, and Fig. 3 demonstrates that our rather simple three-state superposition captures surprisingly well the experimentally observed and ab initio close-coupling results from Fig. 1.

The appearance of the axial vector  $\mathbf{k}_- \times \mathbf{k}_+ = \mathbf{k}_1 \times \mathbf{k}_2$  and the resulting pseudoscalar  $\hat{\mathbf{y}}_M \cdot \hat{\mathbf{k}}_- \times \mathbf{k}_+$  in the description of the molecular state Eq. (7) is a new feature of the  $L > 1$  electron-pair continuum that is not observed in atoms. This special class of molecular fragmentation distributions was recently predicted in general terms [12]. Thus, it would be of interest to try to isolate the axial-vector contributions  $\mathbf{k}_- \times \mathbf{k}_+$  experimentally. Inspection of Eq. (7) shows that these arise in the  $\Pi$  excitation only

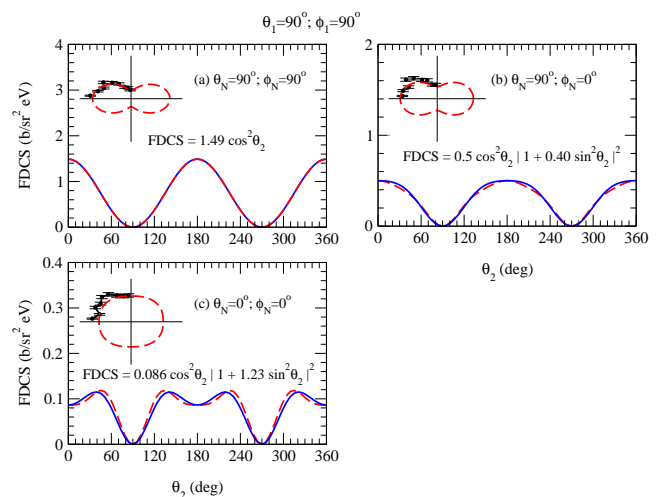


FIG. 3: Fits (solid curves) using Eq. (8) and thus a three-state superposition  ${}^1P_{\lambda=1} + {}^1D_{\lambda=1} + {}^1F_{\lambda=1}$  from Eq. (7) to the  $\text{H}_2$  photo double ionization cross sections in Fig. 1. The dashed curves show the TDCC result from Fig. 1.

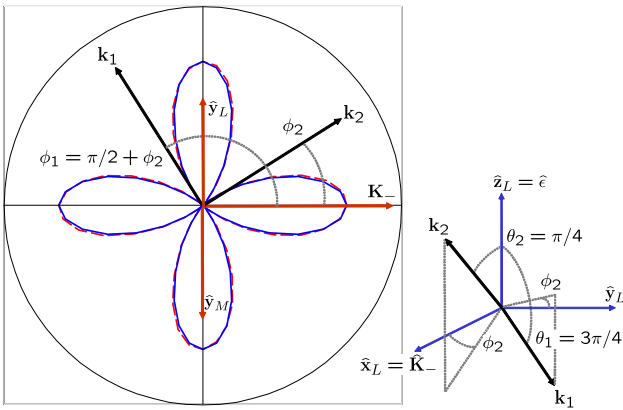


FIG. 4: An electron-pair angular distribution for fixed  $\hat{\mathbf{k}}_1 \cdot \hat{\mathbf{k}}_2$  looking down a  $z_L$  axis along  $\hat{\mathbf{e}}$  onto the  $\hat{\mathbf{x}}_L = \hat{\mathbf{K}}_-$ ,  $\hat{\mathbf{y}}_L$  plane as a function of the azimuthal orientation  $\phi_2$  of the pair. Here,  $\mathbf{k}_2$  and  $\mathbf{k}_1$  are oriented above and below, respectively, the  $\hat{\mathbf{K}}_-$ ,  $\hat{\mathbf{y}}_L$  plane (cf. 3D inset) with fixed polar angles  $\theta_2 = \pi/4$  and  $\theta_1 = \pi - \theta_2$  while varying  $\phi_2$  along with  $\phi_1 = \phi_2 + \pi/2$ . The solid four-lobe curve is the resulting  $\cos^2 2\phi_2$  distribution predicted from the axial-vector contributions to Eq. (7), arbitrarily scaled to a TDCC calculation shown with the dashed curve. The circle radius equals  $0.03 \text{ b/sr}^2 \text{ eV}$ .

and could therefore be extracted by fixing  $\hat{\mathbf{K}}_- \perp \hat{\mathbf{e}}$ , so that  $\cos \theta_N = 0$ , while selecting electron pairs with  $\mathbf{k}_+ \perp \hat{\mathbf{e}}$ . From Eq. (7), one then obtains  $\tilde{\psi}({}^1P_{\lambda=1} + {}^1D_{\lambda=1} + {}^1F_{\lambda=1}) \sim \hat{\mathbf{K}}_- \cdot \hat{\mathbf{k}}_- \hat{\mathbf{y}}_M \cdot \hat{\mathbf{k}}_- \times \mathbf{k}_+$ , as desired. To fix  $\mathbf{k}_+ \perp \hat{\mathbf{e}}$ , one might start with the configuration in Fig. 1b with  $z_L$  axis along  $\hat{\mathbf{e}}$  and  $x_L$  axis along  $\hat{\mathbf{K}}_-$  (so that  $\hat{\mathbf{y}}_L = -\hat{\mathbf{y}}_M$ ) and as depicted in Fig. 4 drop  $\mathbf{k}_1$  in the  $y_L, \hat{\mathbf{e}}$  plane behind  $\mathbf{k}_2$  in the  $\hat{\mathbf{K}}_-$ ,  $\hat{\mathbf{e}}$  plane taking  $\theta_1 = \pi - \theta_2$ . To maintain a frozen-correlation configuration, one can then sweep the electron pair azimuthally about  $\hat{\mathbf{e}}$  keeping  $\hat{\mathbf{k}}_1 \cdot \hat{\mathbf{k}}_2$  fixed by varying the azimuthal angles  $\phi_1, \phi_2$  of  $\mathbf{k}_1, \mathbf{k}_2$  together with say  $\phi_1 = \phi_2 + \pi/2$ . One then obtains the simple angular dependence  $\hat{\mathbf{K}}_- \cdot \hat{\mathbf{k}}_- \hat{\mathbf{y}}_M \cdot \hat{\mathbf{k}}_- \times \mathbf{k}_+ \sim \sin^2 \theta_2 \cos \theta_2 \cos 2\phi_2$  and thus a unique four-lobe angular distribution as a function of  $\phi_2$  [13].

In Fig. 4, we present evidence for this special configuration in the molecular fragmentation cross section calculated with the TDCC theory. One thus finds good agreement with the predicted cross section  $\text{FDSC} \sim \cos^2 2\phi_2$  from the axial-vector contributions to Eq. (7). Besides being relatively weak, we find the distribution to be sensitive to folding over experimental angular acceptances (compare with the insets in Figs. 1 and 3), which quickly mixes back in the competing  $\hat{\mathbf{e}}_{\Pi} \cdot \mathbf{k}_+$  and  $\hat{\mathbf{K}}_- \cdot \mathbf{k}_+$  distributions from Eq. (7) and tends to wash out the four-lobe structure. Nevertheless, one can be hopeful that new experiments in planning with a next-generation light source and upgraded resolution might allow these special geometries in the molecular Coulomb continuum to be identified.

The usefulness of the electron-pair modes defined in

Eq. (4) is the compact description of the continuum spectrum they afford in molecular hydrogen. The same modes, however, should in principle describe *any* low-energy electron-pair continuum. Different systems would in principle only require different sets of mixing coefficients  $a_{L\Lambda\lambda}$ . One hopes to establish in this way a robust and accessible tool for comparing in detail with a variety of existing experimental data. One can thus imagine modeling electron pairs ejected from more complex molecules, and even surfaces and solids, for which ab initio calculations may not exist for some time.

This project has been supported by the Chemical Sciences, Geosciences and Biosciences Division of the Office of Basic Energy Sciences, Office of Science, U. S. Department of Energy. The Los Alamos National Laboratory is operated by Los Alamos National Security, LLC for the National Nuclear Security Administration of the U.S. Department of Energy under Contract No. DE-AC5206NA25396.

\* Electronic address: [jfeagin@fullerton.edu](mailto:jfeagin@fullerton.edu)

- [1] T. J. Reddish and J. M. Feagin, J. Phys. B: At. Mol. Opt. Phys. **32**, 2473 (1999); J. M. Feagin, J. Phys. B: At. Mol. Opt. Phys. **31**, L729 (1998).
- [2] We invoke here the usual *axial-recoil approximation* and make no distinction between the spatial orientation of the molecular axis  $\hat{\mathbf{R}}_N$  and the post-selected relative momentum direction  $\hat{\mathbf{K}}_-$  of the Coulomb exploding ion pair on the heels of the swift electron-pair photoejection.
- [3] M. Gisselbrecht et al., Phys. Rev. Lett. **96**, 153001 (2006).
- [4] Th. Weber et al., Nature (London) **431**, 437 (2004); **443**, 1014 (2006).
- [5] W. Vanroose, F. Martin, T. N. Rescigno, and C. W. McCurdy, Phys. Rev. A **70**, 050703 (R) (2004); Science **310**, 1787 (2005).
- [6] J. Colgan, M. S. Pindzola and F. Robicheaux, J. Phys. B: At. Mol. Opt. Phys. **37**, L377 (2004); Phys. Rev. Lett. **98**, 153001 (2007).
- [7] M. Walter, J. S. Briggs and J. M. Feagin, J. Phys. B: At. Mol. Opt. Phys. **33**, 2907 (2000).
- [8] J. M. Feagin, J. Phys. B: At. Mol. Opt. Phys. **29**, L551 (1996).
- [9] G. Herzberg, *Spectra of Diatomic Molecules*, (2nd Ed., Van Nostrand Reinhold, New York, 1950), Chap. V; R. N. Zare, *Angular Momentum*, (Wiley-Interscience, New York, 1988), Chap. 6.
- [10] This pure  $\cos^2 \theta_2$  dependence persists even if the  ${}^1F_{\lambda=3}$  mode is included in the superposition.
- [11] The  ${}^1P_{\lambda=1}$  and  ${}^1D_{\lambda=1}$  modes in Eq. (7) are degenerate and contribute simply  $\hat{\mathbf{e}}_{\Pi} \cdot \mathbf{k}_+$  in all three cases, Figs. 3a-c.
- [12] M. Walter, A. V. Meremianin, and J. S. Briggs, J. Phys. B: At. Mol. Opt. Phys. **36**, 4561 (2003) and references therein.
- [13] One also obtains a four-lobe angular distribution as a function of  $\theta_2$  for fixed  $\phi_2$ , albeit one with *non-frozen* correlation.